Short communication

Conductive polymer film supporting LiFePO$_4$ as composite cathode for lithium ion batteries

N.D. Trinh, M. Saulnier, D. Lepage, S.B. Schougaard*

Université du Québec à Montréal, Quebec Centre for Functional Materials, Case postale 8888, Succ. Centre-ville, Montréal, Québec, Canada H3C 3P8

HIGHLIGHTS

► Free-standing PEDOT–LiFePO$_4$ composites for lithium ion batteries by dynamic three phase interline electropolymerization.
► PEDOT–LiFePO$_4$ serves as current collector, binder and carbon filler free functional electrodes.
► LiFePO$_4$ mass fraction of 33.5 wt.% in the composite film confirmed by TGA analysis.
► The cathode discharge capacity of the PEDOT–LiFePO$_4$ composite film is 75 mAh g^{-1} at C/10.

ARTICLE INFO

ABSTRACT

Free-standing poly(3,4-ethylenedioxythiophene) (PEDOT)–LiFePO$_4$ composite films were successfully prepared by dynamic three phase interline electropolymerization (D3PIE). These films were used without further modification as the positive electrode in standard lithium ion batteries. As such, this new process eliminates all electrochemically inactive materials (carbon, polymer binder and current collector) used in conventional composite cathodes. The PEDOT–LiFePO$_4$ composite film offers a discharge capacity of 75 mAh g^{-1} at the C/10 rate and high capacity retention at the C/2 rate. When reporting this value to the relative amount of LiFePO$_4$ in the PEDOT-LiFePO$_4$ composite film, the discharge capacity reached 160 mAh g^{-1}, close to the theoretical maximum value (170 mAh g^{-1}). As such, this approach yield highly functional hybrid free-standing conductive polymer/active material composite cathode with controllable size and structure.

© 2012 Elsevier B.V. All rights reserved.

1. Introduction

Lithium ion batteries are used in a wide range of applications from small portable electronic devices to hybrid electric vehicles (HEVs) or electric vehicles (EVs) [1–3]. Among several components in the lithium ion batteries, cathode materials have attracted much attention in recent years [4]. Introduced in 1997 by Padhi et al., *olivine* structured LiFePO$_4$ has emerged as one of the most promising cathode materials for the next generation of lithium ion batteries [5]. LiFePO$_4$ is highly attractive as it is relatively inexpensive and environmentally benign [6]. Further, great stability of this material is provided by the strong covalent P–O bond [5]. However, this material exhibits low ionic and electronic conductivities and tremendous efforts have been made to overcome these

problems [7]. One way to improve the intrinsic problem of low ion diffusivity is downsizing and controlling the morphology of the particle to decrease length of the lithium ion diffusion pathway inside the particle [8,9]. Moreover, several research groups have focused their works on applying a conductive coating such as carbon to the particle surface, so as to increase the electronic conductivity [10–12]. But still a considerable quantity of carbon has to be added to practical composite electrodes to improve their electronic conductivity [13]. This carbon is not electrochemically active, and thus entails a decrease of the practical storage capacity of the cathode.

An alternative way to improve the electronic conductivity is the use of conductive polymers, which show a positive effect on the performance of LiFePO$_4$ [14,15]. In particular, poly(3,4-ethylenedioxythiopene) (PEDOT) is attracting a lot of attention for its conductivity, mechanical flexibility, thermal stability and its ability to improve lithium ion accessibility and the diffusion pathway within battery cathodes [16,17]. Previous works showed

the preparation of a conductive coating by mixing $LiFePO_4$ nanorods in a PEDOT colloidal solution [18]. One particular attractive way to form PEDOT coating consists of using the intrinsic oxidative power of $Li_{(1-x)}FePO_4$ as the driving force for the polymerization [19]. However, to render these particles functional in a battery require the use of a current collector, typically an aluminum foil and a binder, which serves to hold together the particles. Clearly, these components cannot store charge. It would therefore be highly desirable to remove the current collector by developing an ion and electron conductive matrix/electroactive particle composite that is self-contained, *i.e.* free-standing.

Recently, a new method showed the possibility of synthesizing free-standing PEDOT films by dynamic three phase interline electropolymerization (D3PIE) using a biphasic aqueous/organic system, where the electrode is immersed through the interface [20]. The organic dichloromethane phase and aqueous phase contains the monomer and the doping electrolyte (BF_4^-, ClO_4^-, *etc.*), respectively. The electrode is subjected to an oxidative overpotential and the electron, ion and monomer transfer processes operate simultaneously around the electrode to form the polymer film at the aqueous/organic interface. The horizontal size of the polymer is controlled by the reaction time at constant potential. The corresponding PEDOT film shows excellent electronic conductivity and flexibility. Moreover, this method produces in short time (~ 0.1 cm^2 min^{-1}) PEDOT film with high porosity.

In this work, D3PIE method was used to prepare the conductive polymer to support $LiFePO_4$ particles. While the polymer is growing along the interface, it incorporates $LiFePO_4$ particles (density: 3.6 g cm^{-3}) suspended in the aqueous phase (Fig. 1). The significant advantage of this one step technique is that the PEDOT–$LiFePO_4$ films are easily removed from the reactional media and can be used as obtained in standard coin cell batteries.

The PEDOT–$LiFePO_4$ composite films produced in this work were characterized by scanning electron microscopy (SEM) to examine the morphology, thermogravimetric analysis (TGA) to determine the PEDOT–$LiFePO_4$ ratio, while electrochemical performance of PEDOT–$LiFePO_4$ films was examined using chronopotentiometry.

2. Material and methods

3,4-Ethylenedioxythiophene (EDOT) (AK Scientific 99%), dichloromethane (CH_2Cl_2) (EMD Chemical Grade ACS) and tetraethylammonium tetrafluoroborate ($TEABF_4$) (Alfa Aesar 99%) were used as received. Commercial grade $LiFePO_4$–C was generously donated by Phostech Lithium Inc. (St-Bruno-de-Montarville,

Canada). The $LiFePO_4$ sample was dried at 60 °C under vacuum overnight before analysis.

Electropolymerization at constant potential was performed using a Bio-Logic VMP3 potentiostat. The reference electrode was Ag/AgCl (3 M NaCl) (Basi) and the counter electrode consisted of reticulated vitreous carbon (RVC) foam, 3% density (ERG Materials and Aerospace Corp.) with a porosity of 30 PPI connected to a platinum wire. A 0.9 mm diameter graphite rod served as working electrode and was vertically immersed into the water/dichloromethane solution. The reference and counter electrode were immersed only in the aqueous phase. An aqueous solution of 0.1 M $TEABF_4$ and a 0.1 M EDOT in dichloromethane solution were used to prepare PEDOT films. For the PEDOT–$LiFePO_4$ films, a 5 wt-% $LiFePO_4$/0.1 M $TEABF_4$ in H_2O suspension solution was prepared and sonicated during 10 min to eliminate aggregates. The solution was poured on the organic phase and the $LiFePO_4$ particles slowly decanted to cover the entire water/dichloromethane interface. The reaction lasted 30 min at a constant potential of 1.3 V *vs.* Ag/AgCl (3 M NaCl) to obtain a disk shaped film with an approximate diameter of 1 cm. The PEDOT-$LiFePO_4$ films were washed by deionised water (5 × 10 mL) followed by acetonitrile (5 × 10 mL). The films were dried at 60 °C under vacuum overnight, before further use.

The morphology of the PEDOT–$LiFePO_4$ films was determined by a JEOL JSM840 scanning electron microscopy using an SEI detector and 5.0 kV acceleration voltage. Thermogravimetric analyses were performed under air using a Seiki Instrument Inc. TG/DTA6200 (temperature profile: 30–600 °C (3 °C min^{-1}); 600 °C (60 min); 600–30 °C (6 °C min^{-1}). The conductivity measurement was performed by the Van der Pauw method using a homemade measuring station (Keithley system: 7001 switch system, 6220 precision current source and 2000 multimeter) [21]. The thickness of the composite film was measured by a Mitutoyo 7326S thickness gage. The electrochemical performances of PEDOT–$LiFePO_4$ films were determined with CR2032-type coin cells using metallic lithium (Alfa Aesar 99.9%) as the anode. The electrolyte was 1 M $LiPF_6$ in a 1:1 ethylene carbonate (EC) and dimethyl carbonate (DMC) mixture (Novalyte Technologies) and Celgard 2500 was used as the separator. The cells were assembled in an argon atmosphere glove box (H_2O < 1 ppm, O_2 < 1 ppm).

Electrochemical testing was performed by galvanostatic cycling with the voltage range of 2.2–4.2 V *vs.* Li/Li^+ at room temperature using a BST8-MA 8 channels battery analyzer. An open circuit rest period was imposed during 1 h after every charge/discharge process. Electrochemical impedance spectroscopy (EIS) was performed using a Bio-Logic VMP3 potentiostat on PEDOT-$LiFePO_4$ composite film at a series of fixed potentials between 2.2 and 4.2 V *vs.* Li/Li^+. The coin cell battery was charged at constant current of C/5 until reaching the desired potential. Then, the voltage was kept constant until the current fluctuation was lower than 0.01 mA (~ 4 h). AC amplitude of 5 and 10 mV was applied in a frequency range of 100 kHz–0.01 Hz. Spectra collected with 5 *vs.* 10 mV were identical within the experimental error (<1%).

3. Results and discussion

3.1. Electropolymerization of PEDOT and PEDOT–$LiFePO_4$ films by chronoamperometry

Fig. 2 shows the current–time profiles of the electropolymerization of PEDOT and PEDOT–$LiFePO_4$ films by chronoamperometry. As the polymer grows, the charge transfer occurs at the circumference of the formed PEDOT film. The PEDOT–$LiFePO_4$ sample shows higher current compared to pure PEDOT for the duration of the polymerization. This is expected as $LiFePO_4$
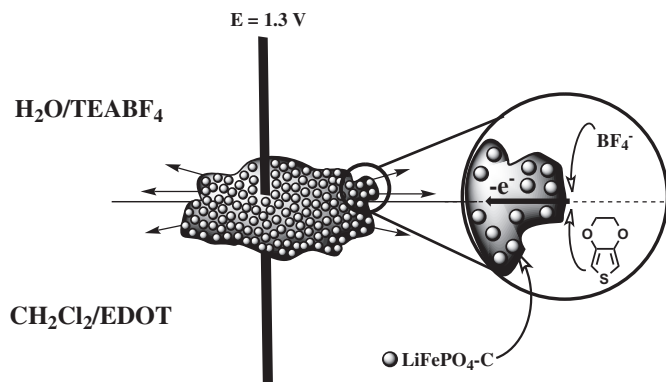

Fig. 1. Schema of the D3PIE method in dynamic growth with $LiFePO_4$ at the water/dichloromethane interface.
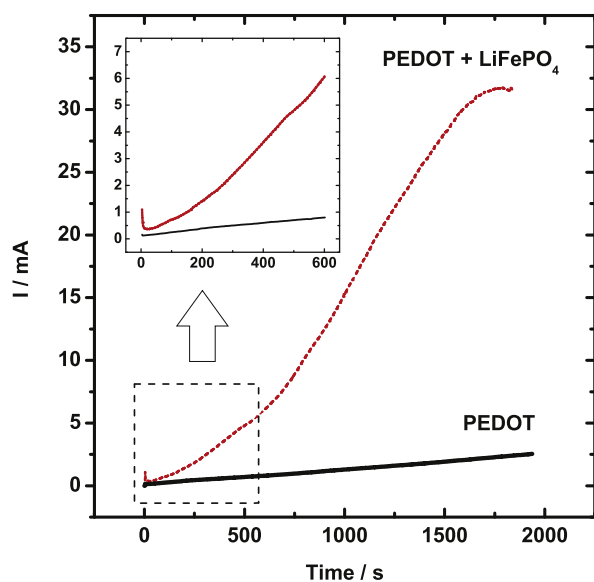
Fig. 2. Current–time profiles for electropolymerization of PEDOT at constant potential, from 1.3 V *vs.* Ag/AgCl (3 M NaCl) in 0.1 M TEABF$_4$ in H$_2$O/0.1 M EDOT in CH$_2$Cl$_2$ (−) and 5% LiFePO$_4$ in 0.1 M TEABF$_4$ in H$_2$O/0.1 M EDOT in CH$_2$Cl$_2$ (---). In inset, the current–time profiles for the first 10 min.

particles included in the conductive polymer will undergo at least partial oxidation, and thus contribute to the current profile. When the polymerization last for more than 30 min, the film thickness starts to increase while diameter cease to augment. At this point, the polymer has vertical preferential growth. It is supposed that this phenomenon is caused by the ohmic drop between the electrode and the radial point of the film. The typical PEDOT film conductivity was 5.8 S cm^{-1}, as obtained by the four-points probe technique.

3.2. Morphology of the PEDOT and PEDOT–LiFePO$_4$ films

The choice of doping electrolyte is important, as it influences the morphology strongly [20]. Utilization of ClO$_4^-$ anion inverses the morphology compared to BF$_4^-$ anion, *i.e.* for ClO$_4^-$ the organic phase side showed great porosity while the aqueous phase showed a smooth/dense morphology.

SEM micrographs of PEDOT and PEDOT–LiFePO$_4$ films doped with BF$_4^-$ anion (Fig. 3) reveal the microstructure, of the side toward the organic phase, to be a dense microglobular film with low porosity. Inversely, for the side toward the aqueous phase, a highly porous morphology with many cavities present throughout the surface. This morphology of the polymer structure is ideal for polymerizing PEDOT in the presence of LiFePO$_4$ particles. A highly

porous polymer allows more LiFePO$_4$ particles to be included in the film, which translates into an increase of the energy density. Moreover, the high porosity facilitates the accessibility for the electrolyte.

Fig. 4 shows the aqueous phase of (a) PEDOT and (b) PEDOT–LiFePO$_4$ films doped with the BF$_4^-$ anion. In Fig. 4 (a), the polymer clearly demonstrates the porosity of the aqueous phase. The pores size varies between less than a micron to ∼5 μm of diameter. Well-dispersed individual LiFePO$_4$ are clearly visible around the micropores in Fig. 4 (b). Fig. 4 (c) shows the side toward the organic phase and demonstrates smooth edges of the pores. Importantly, LiFePO$_4$ particles were included differently on this side compared to the aqueous side of the PEDOT film (Fig. 4 (d)). In this case, the LiFePO$_4$ particles were attached to the smooth edges without incorporation into the polymer. The average thickness of the composite film was ∼350 μm and the total weight per area is 2.3 mg cm^{-2}.

3.3. Thermogravimetric analyses

To quantify the amount of LiFePO$_4$ in PEDOT–LiFePO$_4$ composite film, thermogravimetric analyses were undertake for PEDOT, LiFePO$_4$ particles and PEDOT–LiFePO$_4$ under oxidizing (air) condition (Fig. 5). The 1.5% gain of weight for LiFePO$_4$ is due to the oxidation of LiFePO$_4$. In comparison, PEDOT suffers a 100% mass loss due to its reaction into volatiles molecules. The amount of LiFePO$_4$ in PEDOT–LiFePO$_4$ composite film is therefore directly related to the difference between these samples. As such, the 35 wt.% residual mass for the PEDOT–LiFePO$_4$ sample corresponds to a LiFePO$_4$ mass fraction of 33.5 wt.%.

3.4. Electrochemical performance of PEDOT and PEDOT–LiFePO$_4$ films

Electrochemical performances were evaluated using standard coin cells. PEDOT and PEDOT–LiFePO$_4$ films were used directly as the cathode without aluminum current collector, binder or carbon additive. Fig. 6 (a) shows the charge/discharge profile of PEDOT film at a C/5 constant current rate in the 2.2–4.0 V *vs.* Li/Li$^+$ voltage range. A cathode discharge capacity of 16 mAh g^{-1} was obtained, which remained constant (±7%) during more than 75 cycles (Fig. 6 (b)); this confirms the stability of the polymer in the battery environment.

Fig. 7 (a) compares the voltage profile of PEDOT–LiFePO$_4$ film at different discharge rate of C/10 to 5C, using a fixed charge rate of C/10. As expected, the electrode capacity is improved by incorporating LiFePO$_4$ particles into the PEDOT film. The PEDOT–LiFePO$_4$ film exhibits a cathode discharge capacity of 75 mAh g^{-1} with little difference between the charge and discharge curve at C/10 rate in the voltage range of 2.2–4.2 V *vs.* Li/Li$^+$. By reporting this
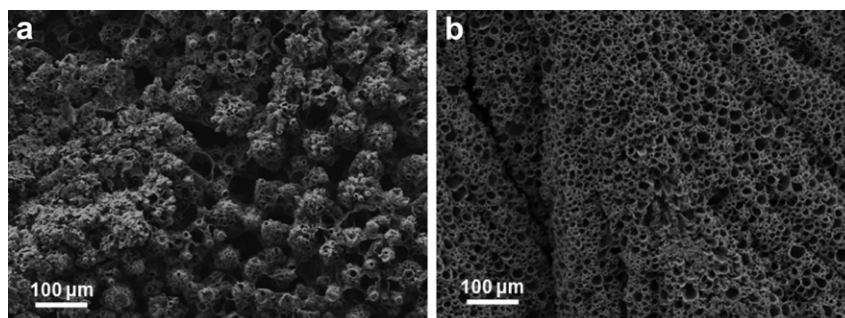

Fig. 3. SEM micrographs at 150× of PEDOT film of the side toward the (a) organic phase and (b) aqueous phase prepared at constant potential.
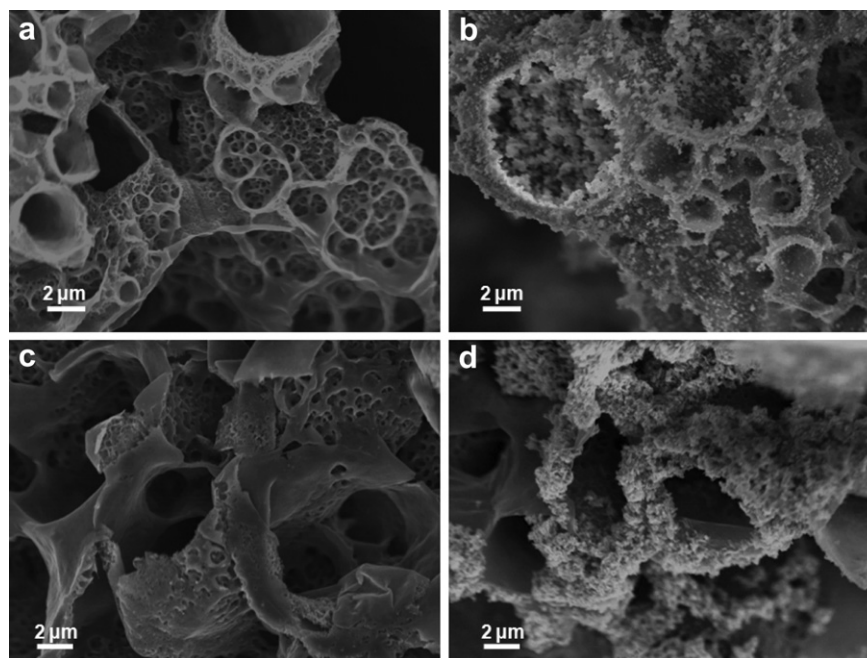
Fig. 4. SEM micrographs of the side toward the aqueous and organic phases of PEDOT (a,c) and PEDOT−LiFePO$_4$ (b,d) films prepared at constant potential of 1.3 V *vs.* Ag/AgCl (3 M NaCl).

value relative to the amount of LiFePO$_4$ in the PEDOT−LiFePO$_4$ composite film, the discharge capacity reached∼160 mAh g^{-1}, close to the theoretical maximum value of 170 mAh g^{-1}. To compare the practicality of the PEDOT−LiFePO$_4$ composite film, we compare the capacity to conventional thin-film composite electrodes deposited onto aluminum current collectors. The coating composition includes binder and carbon additive, as well as the active material, in relative ratios, which depend on the application. However, typically the active material constitutes 80−90% of the mass [22]. The thickness and the density of the coatings also vary according to application; yet, typical loadings are in the 10.8−13.2 mg cm^{-2} range for a 60 μm LiFePO$_4$ electrode. Assuming a typical aluminum current collector thickness of 30 μm [22] this means that the active material constitutes 31−48% of the total electrode mass depending on the coating thickness (30−60 μm).

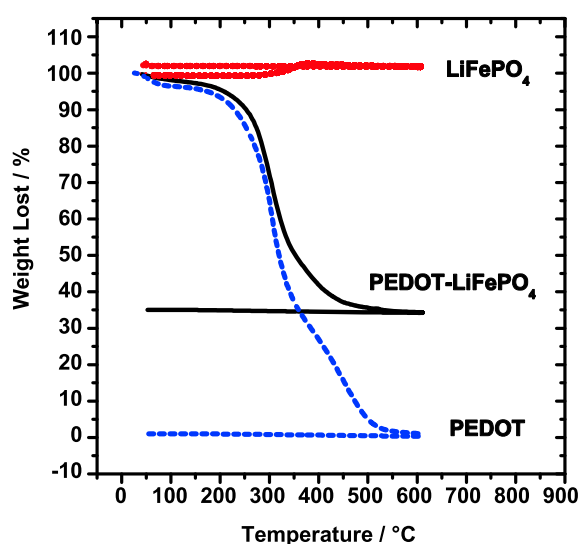**Fig. 5.** Thermograms of PEDOT (---), LiFePO$_4$ (•••) and PEDOT−LiFePO$_4$ (—). Analysis parameters: 30−600 °C (3 °C min^{-1}); 600 °C (60 min); 600-30 °C (6 °C min^{-1}).

These values are equivalent to our PEDOT−LiFePO$_4$ composites, without having completed any optimization of the process.

The discharge curve (C/10) at Fig. 7 (a) clearly shows a plateau at 3.4 V *vs.* Li/Li$^+$, as is found for the reinsertion of Li$^+$ into Li$_{(1-x)}$FePO$_4$ [23]. After the apparent plateau, the curve slowly decreases, similar to the voltage profile curve of the PEDOT during lithium ions reinsertion. Interestingly, at constant current rate of discharge of 1 h (C), the PEDOT−LiFePO$_4$ film still exhibits a 69% discharge capacity retention compared to the value at the C/10 rate. Importantly the electrochemical tests were performed without adding carbon or binder to the electrode.

For faster discharge rates (C and 5C), the plateau slowly disappears most likely due to transport limitation [22]. Fig. 7 (b) shows the cyclability of the PEDOT−LiFePO$_4$ film at C/2 rate. The cathode discharge capacity remained virtually unchanged after 50 cycles, revealing a good stability of the material.

Unlike the standard carbon particle/polymer binder matrix, the electronic conductivity of PEDOT is dependent on the electrochemical potential [24]. Specifically, the undoping of the polymer at reducing potentials will lead to an insulating behaviour. We therefore studied the electronic conductivity at different potentials by electrochemical impedance spectroscopy (EIS) for PEDOT−LiFePO$_4$ composite film. Importantly, since the electrochemical reaction takes place throughout the thickness of the electrodes, the electronic conductivity of the polymer has profound effect on R_{ct}. Importantly, R_{ct} is only marginally affected by the electrochemistry of LiFePO$_4$ at potentials above and below the standard potential for the LiFePO$_4$ insertion/desinsertion reaction (3.4 V *vs.* Li/Li$^+$) [23]. Instead, R_{ct} is dominated by the oxidation/reduction of the polymer. The simplified contact-Randles-film circuit (SCRF) [25] shown in the inset of Fig. 8 (a) was used to analyse the impedance spectra of the PEDOT−LiFePO$_4$. The model proposes significance for the selected circuit parameters and is experimentally verified using carefully modeled experiments of LiFePO$_4$ material. Qualitatively, Fig. 8 (a) shows semicircle for impedance measured at the high frequencies, commonly associated with the charge transfer resistance (R_{ct}). At lower frequencies, the typical diffusion limited Warburg behaviour is observed. The equivalent circuit simulated
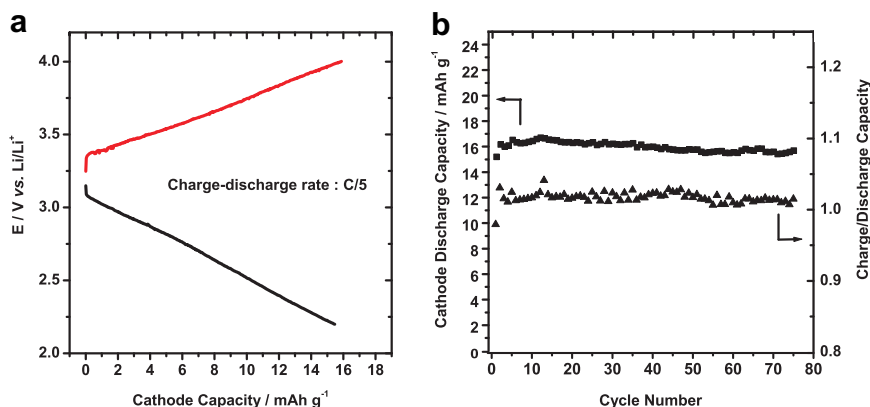
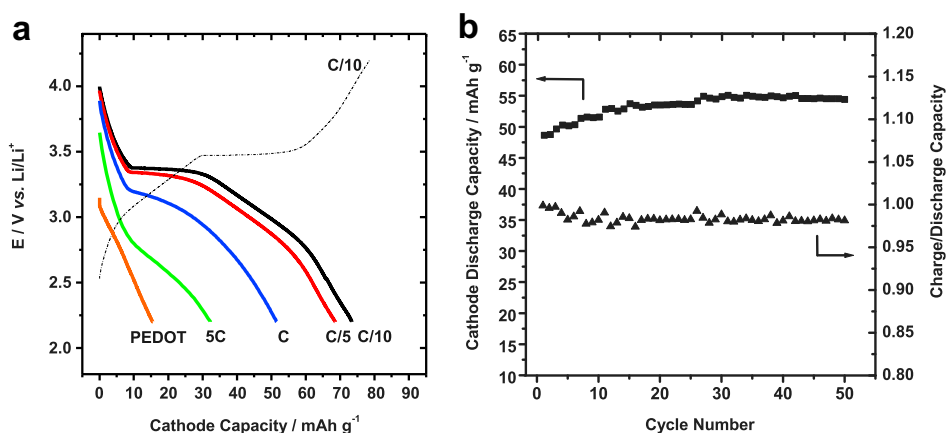**Fig. 6.** (a) Charge—discharge profiles at C/5 rate and (b) cyclability of the PEDOT film.

Fig. 7. (a) Comparison of different rate capabilities and (b) cyclability at C/2 rate of PEDOT—LiFePO$_4$ film.
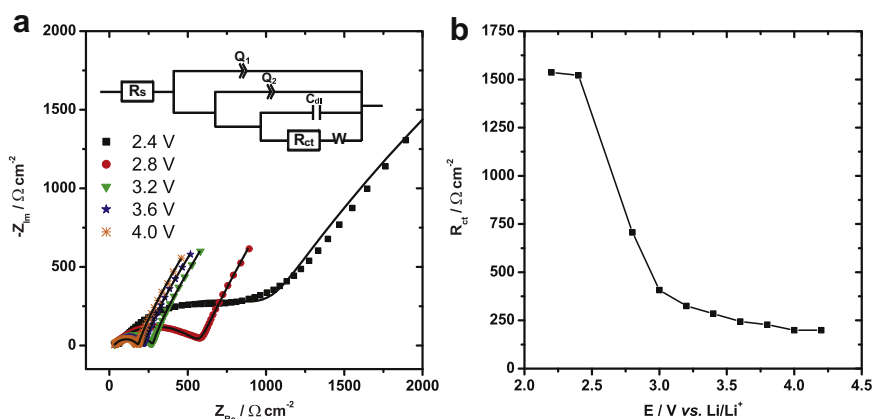

Fig. 8. (a) Impedance spectra for the PEDOT—LiFePO$_4$ film at different potentials (solid line: simulated data). In inset, the equivalent circuit for the electrode. (b) charge transfer resistance at different potentials.

electrochemical parameters are in good agreement with the experimental results. Fig. 8 (b) shows the charge transfer resistance values obtained at different potentials. The R_{ct} values between 4.2 and 3.0 V *vs.* Li/Li$^+$ remain relatively constant between 200 and 330 Ω cm^{-1}, revealing that the conductive polymer efficiently transport charge in his voltage range. Below 3.0 V *vs.* Li/Li$^+$, R_{ct} drastically increases by a factor of 5. We explain this behaviour by a reduction/undoping of the polymer PEDOT, which leads to a poorly conducting polymer below 3.0 V [24]. Importantly, this

potential threshold is well below the operating voltage of LiFePO$_4$ and should therefore not affect performance.

4. Conclusion

In this work, free-standing PEDOT—LiFePO$_4$ films were successfully prepared by D3PIE method. The PEDOT provides mechanical support for the incorporated LiFePO$_4$ particles. This technique is interesting as the composite films are easily removed

from the reactional medium and can be used directly as the cathode in lithium ions batteries. Moreover, the electrochemical inactive materials required in conventional composite cathodes have been eliminated. The electrochemical measurements demonstrate that the PEDOT−LiFePO$_4$ film achieves a discharge capacity of 75 mAh g^{-1} at the C/10 rate and exhibits excellent cyclability in lithium cells. The high discharge capacity of $\sim$160 mAh g^{-1} is preserved when referring to the relative amount of LiFePO$_4$ in PEDOT−LiFePO$_4$ film. The preliminary results reported here open a new avenue to explore the development of ionic/electronic conducting support structures for LiFePO$_4$ particles.

Acknowledgement

References

[1] D.A. Notter, M. Gauch, R. Widmer, P. Wager, A. Stamp, R. Zah, H.J. Althaus, Environ. Sci. Technol. 44 (2010) 6550–6556.
[2] E. Karden, S. Ploumen, B. Fricke, T. Miller, K. Snyder, J. Power Sources 168 (2007) 2–11.
[3] H. Li, Z. Wang, L. Chen, X. Huang, Adv. Mater. 21 (2009) 4593–4607.
[4] J.W. Fergus, J. Power Sources 195 (2010) 939–954.
[5] A.K. Padhi, K.S. Nanjundaswamy, J.B. Goodenough, J. Electrochem. Soc. 144 (1997) 1188–1194.
[6] Y. Wang, P. He, H. Zhou, Energy Environ. Sci. 4 (2011) 805–817.
[7] M. Park, X. Zhang, M. Chung, G.B. Less, A.M. Sastry, J. Power Sources 195 (2010) 7904–7929.
[8] P. Bruce, B. Scrosati, J.-M. Tarascon, Angew. Chem. Int. Ed. 47 (2008) 2930–2946.
[9] Y. Wang, H. Li, P. He, E. Hosono, H. Zhou, Nanoscale 2 (2010) 1294–1305.
[10] Y.-H. Huang, K.-S. Park, J.B. Goodenough, J. Electrochem. Soc. 153 (2006) A2282–A2286.
[11] N. Ravet, Y. Chouinard, J.F. Magnan, S. Besner, M. Gauthier, M. Armand, J. Power Sources 97-98 (2001) 503–507.
[12] H.C. Shin, W.I. Cho, H. Jang, Electrochim. Acta 52 (2006) 1472–1476.
[13] R. Dominko, M. Gaberscek, J. Drofenik, M. Bele, S. Pejovnik, J. Jamnik, J. Power Sources 119-121 (2003) 770–773.
[14] G.X. Wang, L. Yang, Y. Chen, J.Z. Wang, S. Bewlay, H.K. Liu, Electrochim. Acta 50 (2005) 4649–4654.
[15] K.-S. Park, S.B. Schougaard, J.B. Goodenough, Adv. Mater. 19 (2007) 848–851.
[16] L. Zhan, Z. Song, J. Zhang, J. Tang, H. Zhan, Y. Zhou, C. Zhan, Electrochim. Acta 53 (2008) 8319–8323.
[17] H.-C. Dinh, S.-i. Mho, I.-H. Yeo, Electroanalysis 23 (2011) 2079–2086.
[18] A. Vadivel Murugan, T. Muraliganth, A. Manthiram, Electrochem. Commun. 10 (2008) 903–906.
[19] D. Lepage, C. Michot, G. Liang, M. Gauthier, S.B. Schougaard, Angew. Chem. Int. Ed. 50 (2011) 6884–6887.
[20] H. Zhu, L. Gao, M. Li, H. Yin, D. Wang, Electrochem. Commun. 13 (2011) 1479–1483.
[21] L.J. Van der Pauw, A Method of Measuring Specific Resistivity and Hall Effects of Discs of Arbitrary Shape, Philips Res. Repts., 13 (1958): 1.
[22] D.Y.W. Yu, K. Donoue, T. Inoue, M. Fujimoto, S. Fujitani, J. Electrochem. Soc. 153 (2006) A835–A839.
[23] C. Delmas, M. Maccario, L. Croguennec, F. Le Cras, F. Weill, Nat. Mater. 7 (2008) 665–671.
[24] H.J. Ahonen, J. Lukkari, J. Kankare, Macromolecules 33 (2000) 6787–6793.
[25] J.-M. Atebamba, J. Moskon, S. Pejovnik, M. Gaberscek, J. Electrochem. Soc. 157 (2010) A1218–A1228.